Theoretical and Applied Fracture Mechanics 111 (2021) 102848

Contents lists available at ScienceDirect

Theoretical and Applied Fracture Mechanics

journal homepage: www.elsevier.com/locate/tafmec

Residual stress estimation in defect assessment procedures at weld toe and away locations on girth welds: Review of key parameters

Sachin Bhardwaj *, R.M. Chandima Ratnayake

Department of Mechanical and Structural Engineering and Materials Science, University of Stavanger, N-4036 Stavanger, Norway

ARTICLE INFO

Keywords:
Residual stress
Girth welds
BS 7910
API 579
Structural integrity

ABSTRACT

The distribution of residual stresses in welded joints plays an important role within the fracture evaluation guidelines recommended in structural integrity assessment codes such as BS7910, API 579 RP-1/ASME FFS-1 and R6. The residual stress profile recommendations in these standards are based on extensive experimental results and finite element modelling (FEM) based parametric residual stress evaluations at the weld centerline and weld toe positions. The upper bound residual stresses' profiles based on these recommendations vary significantly from one type of welding process to another for a given weld configuration with identical welding conditions. These fitness-for-service codes (FFS) depict great variability in estimating residual stress profiles during defect assessment, as BS 7910 & R6 recommends a constant profile at a distance away from welds and API 579 provides a single curve for all locations in the axial direction. Thus, conservatism is widely associated with these recommended profiles in fracture potential evaluation and assessments, leading to suboptimal recommendations. In this manuscript, a detailed review is undertaken of residual stress estimation in various FFS codes, showing vast variability among them for locations away from the weld toe on girth welds. Key distinct parameter characteristics, pipe radius to thickness ratio and heat input are detailed and found to have a significant effect on residual stress profiles in structural integrity assessment, using a stress decomposition technique. These recommendations establish an overall analysis of the interrelationship between key parameters, considering a generalized broad range of applications. A framework is proposed, based on the current review, for conducting detailed investigation by employing thermomechanical numerical modelling, coupled with measurement results (nondestructive and semi-destructive) from an experimental study, as input to machine-learning algorithms for application guidance to engineers.

1. Introduction

1.1. Background

Welding and its application constitute one of the most varied and extensively used mechanical joining processes in the offshore structure and piping industry [1–4]. In an offshore and piping structure, weld joint fabrication in piping is carried out through different welding processes and welding procedure specifications (WPSs), comprising various essential and non-essential welding parameters [5]. Due to their compact layout and offshore jacket, primary (TKY) weld joints often face the challenge of maintaining a minimum distance between proximity welds [6]. Due to the lack of clarity in various fabrication codes regarding maintaining these distances, various challenges, such as the development of harmful tensile residual stresses, microstructural and strength changes in the heat affected zone (HAZ) as a result of varying cycles of heating and cooling etc., develop between proximity welds [6–8]. Varying cycles of heating and cooling can give rise to high residual stress between proximity welds, requiring the correct estimation of residual stresses in fitness-for-service codes at distances away from the weld [6,9]. In the failure assessment of such structures, residual stresses are found to have a deleterious effect on the structural integrity of welded joints, due to the presence of harmful tensile residual stress in weld toe or root locations, which helps in crack propagation, thus reducing the fatigue life of joints under cyclic loading [10].

High tensile stress at the root region helps to accelerate stress corrosion cracking in the case of corrosive fluid contact with weld root regions [11,12]. Residual stresses are internal self-equilibrating secondary stresses, which are inherent in structures because of the manufacturing process, welding process, restraint, etc. and are difficult to determine or calculate during defect assessment [13]. Hence, correct

* Corresponding author.
E-mail address: sachin.bhardwaj@uis.no (S. Bhardwaj).

https://doi.org/10.1016/j.tafmec.2020.102848
Received 3 August 2020; Received in revised form 20 October 2020; Accepted 25 November 2020
Available online 1 December 2020

Nomenclature

σ_m^r	membrane component of residual stress MPa	tn	weld pass layer thickness in mm
σ_b^r	bending component of residual stress MPa	$Q_1^{'}$	heat content involved to deposit a molten weld pass at a specified melting temperature in J/mm
$\sigma_{s.e}^r$	self-equilibrating component of residual stress MPa	$Q_2^{'}$	heat that is required to hold the melting temperature in J/mm
σ_y	yield strength in MPa	t_{hold}	hold time in sec
K	stress intensity factor	ρ	material density
t	thickness of pipe in mm	Cp	specific heat
x	distance from inside of pipe to outside of pipe in mm	$Apass$	averaged cross section weld pass area in mm^2
Q'	linear heat input in J/mm	k	thermal conductivity
I	welding current in Amp	α	thermal diffusivity
V	welding voltage in volts	$Lsurf$	weld pass surface contacted to the surroundings
u	welding travel speed in mm/sec	ΔT	temperature difference, temperature change from room temperature to the prescribed weld metal temperature
r	mean pipe radius in mm		
$\dot{Q}$	characteristic heat input in J/mm^2	ε	dimensionless factor

estimation in the structural integrity assessment of welded joints becomes a major part of fitness-for-service codes. Correct estimation of residual stresses is essential during defect assessment of weld joints in fitness-for-service codes (FFS) and standards like BS7910-2019, API 579 RP-1/ASME FFS-1 and R6 [14–18]. In these FFS codes, residual stress profile estimation is prescribed, based either on results from available experimentation measurements or finite element (FE) -based parametric residual stress solutions [19]. In FFS codes for welded joints, defect assessment generally follows three approaches, the first of which is the most conservative and the last the most realistic [20]:

(I) approximating tensile residual stress to be uniformly distributed which are equal in magnitude to the mean material yield strength,
(II) upper-bound profiles based on experimental and numerical residual stress results, recommended by various codes, and
(III) nonlinear finite element modelling results coupled with residual stress experimental measurements.

Upper bound profiles available in these FFS codes for residual stress estimation are generally available for location at weld centerline or weld toe in through-thickness transverse and hoop directions, as shown in Figs. 1 and 4.

1.2. Existing challenges in residual stress assessments of welded joints at a distance away from the weld

Residual stress through-thickness estimation at distances away from the weld is practically nonexistent in these FFS codes, which can result in overly conservative assessments when applying fracture mechanics-based structural integrity procedures [21]. During the defect assessment of regions in the proximity of welded joints [6] and residual stress-induced stress corrosion cracking in tube sheet welds [19,21,22], residual stress upper bound profiles at a distance away from the weld become important and information of which is not available in these FFS codes. Moreover, the available upper bound profiles in FFS codes [14–18] have been found to show drastic inconsistencies, considering different welding processes, weld geometries and weld joint configurations [23]. This is primarily due to the complex nature of welding, variability in various available finite element models and the different

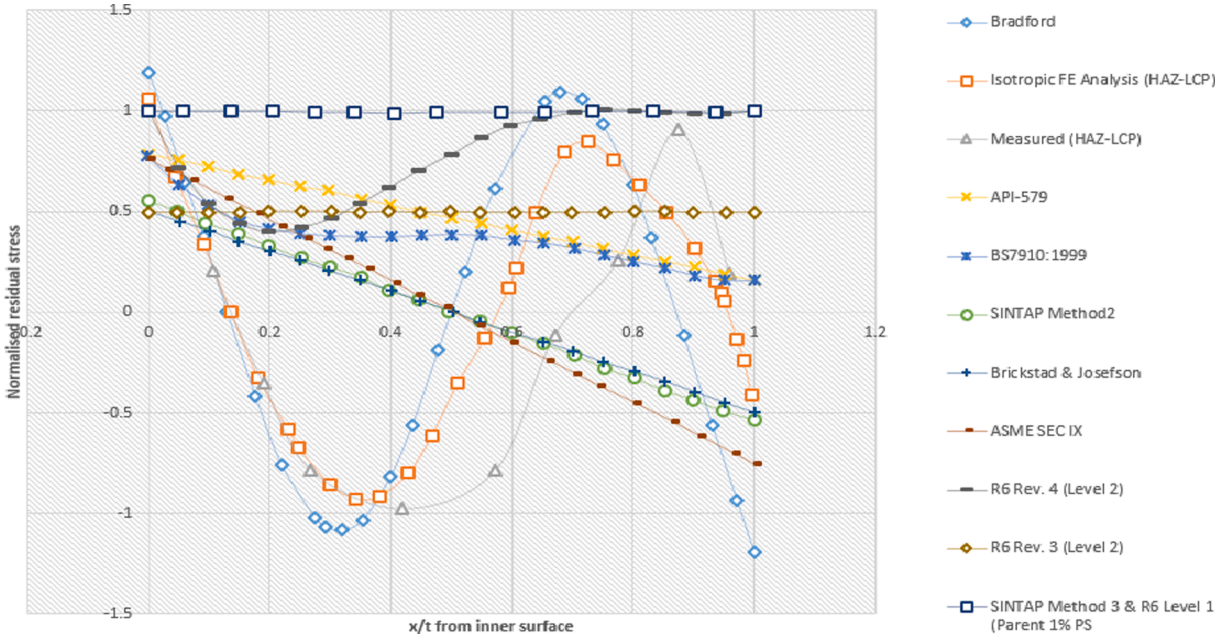

Fig. 1. Comparison, from current codes and recommended assessment procedures, of residual stress profiles in axial direction for a pipe girth weld; adapted from [23].

techniques available for residual stress measurement [24,25]. Fig. 1 illustrates variation in different residual stress distributions from various codes and recommended procedures for the same joint configuration and welding conditions [23].

Upper bound profiles prescribed in FFS codes, as shown in Figs. 1 and 4 for BS7910, are based on polynomial curve fits on selected welded components [14,16,18], supplemented with finite element results [26]. However, recent research has demonstrated that residual stress estimation profiles at a distance away from the weld can be significant, where component geometry pipe radius to thickness ratio (r/t) [27–29] and heat input [19,21,22] are identified as distinct parameters. Residual stress profiles in FFS codes are determined in terms of circumferential girth welds and longitudinal seam welds. For girth welds, the 2007 API RP 579 [30], provides a single curve-based upper bound profile for all distances away from the welds in the axial and hoop directions [21]. In longitudinal seam welds, guidance provided by FFS codes are limited in scope for residual stress profile estimation in defect assessment. In BS7910 [18] and R6 [16], the transverse residual stress profile remains the same over a circumferential distance of 1.5 W from the weld centerline, where W is the seam weld width, as shown in Fig. 5. BS 7910 [18] gives no guidance for locations beyond 1.5 W, and R6 [16] assumes a linear reduction to zero at a small distance.

FFS codes like BS 7910 [18] Annex Q consider the effect of heat input on girth welds by recommending three different profiles: 'high' (heat input $>$ 120 J/mm2), 'low' (heat input $\leq$ 50 J/mm2) and 'medium' (heat inputs between 50 and 120 J/mm2) [31]. BS7910 also follows the partitioning of polynomial distributions' [20] upper bound curve into decomposed components of membrane, bending and self-equilibrating from stress decomposition procedure [32], based on finite element parametric stress analysis results and validated experimentally on selected components by many researchers [23,32]. This decomposition technique helps in determining less conservative non-linear residual stress distribution in the pipe girth welds, decomposing them into global bending, local bending, and self-equilibrating components [20].

With this background, it is evident that residual stress profiles in these FFS codes contain practically no recommendations for locations far from the weld center, where fracture assessment can have a deleterious effect on structural integrity. Conservatism is widely associated with these FFS codes [22,26]; hence, distinct parameters like pipe r/t ratio and heat input role require detailed explanation in determining residual stress profiles for locations at weld center / weld toe and at a distance away from welds. Firstly, this manuscript briefly presents a comparison of residual stress profiles in various structural integrity codes at the weld center and at a distance away from the weld. Thereafter, it discusses in detail the role of distinct parameter characteristics such as pipe r/t ratio and heat input in the evaluation and assessment of piping girth weld residual stress profiles using the stress decomposition technique. Finally, it provides a brief review of a shell theory-based estimation scheme to be introduced in API/ASME Fitness-for-Service Joint Committee recommendations for determining consistent residual stress profiles. These recommendations establish an overall analysis of the interrelationship between key parameters, considering a generalized broad range of applications. Such analysis enables less conservative estimation criteria to be developed for the residual stress evaluation at a distance away from the weld and its assessment, to complement the current approaches suggested in structural integrity. Based on the current review, a framework, Appendix A, is proposed for conducting detailed investigation by employing thermo-mechanical numerical modelling, coupled with measurement results (nondestructive and semi-destructive) from an experimentation study as input to machine-learning algorithms for application guidance to engineers. Beneficial input parameter selection can be made by back propagation techniques, based on the accuracy of predicting residual stress from surrogate models in the front feed direction.

1.3. Stress decomposition technique

Residual stress distribution in welded joints typically consists of both high tensile and compressive stresses, as shown in Fig. 2. These stresses can have a magnitude equal or close to the yield strength of the component. However, their location, magnitude and distribution largely depend on weld joint geometry, the welding process, material characteristics and restraint condition. With this in mind, Dong and his co-workers [32,33] introduced a length scale-based characterization known as a stress decomposition technique. In this technique, residual stress through-thickness profiles are decomposed into stress components of membrane, bending and self-equilibrating stress, which are in decreasing length scale, as shown in Fig. 2 [32]. This stress decomposition is based on the following equations.

$$\sigma_m^r = \frac{1}{t}\int_0^t \sigma^r(x)dx \tag{1}$$

$$\sigma_b^r = \frac{6}{t^2}\int_0^t \sigma^r(x)\left(\frac{t}{2}-x\right)d \tag{2}$$

$$\sigma_{s.e}^r = \sigma^r(x) - \sigma_m^r - \sigma_b^r\left(1-\frac{2x}{t}\right) \tag{3}$$

An example of this technique on a T fillet weld transverse residual stress by finite element analysis is shown in Fig. 2, depicting the decreasing length scale [32], where x varies from the inside to the outside of the pipe of thickness t.

It is worth mentioning here that Eqs. (1)–(3) represent through thickness self-equilibrating stress distribution, highlighting the decreasing length scale of residual stress distributions in the form of membrane, bending, and self-equilibrating stress, with respect to the thickness t. This technique also separates the contribution of global (due to membrane and bending stresses) and local residual stress (due to self-equilibrating stress) components, which can help in estimating the stress intensity factor K, due to residual stresses [24]. The membrane component σ_m^r and the bending component σ_b^r play an important role in defect assessment procedures to estimate the fracture crack driving force and are well demonstrated in the work of Dong and his co-workers [19,34]. In addition, this technique also helps in visualizing clear and better patterns of residual stress distribution and in analyzing many residual stress cases, to identify the controlling parameters.

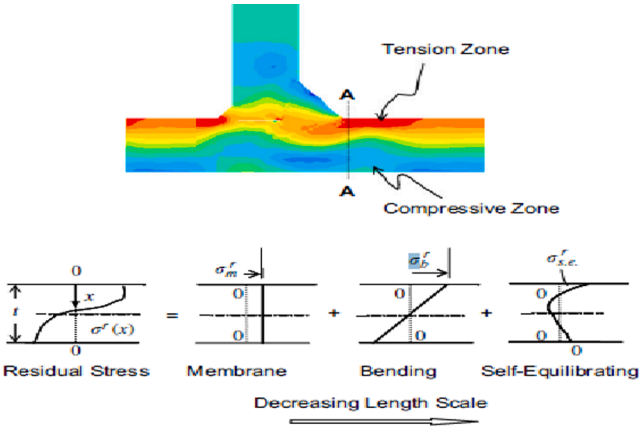

Fig. 2. Illustration of residual stress decomposition technique components with decreasing length scale [32] .

1.4. Scopes and objectives

- Carry out a brief review of the guidance on residual stress profiles for assessing flaws in as-welded joints recommended in Annex Q of BS 7910, API 579 and R6 for girth welds locations at the weld center/ weld toe and at distances away from welds.
- Review of important parameters that govern residual stress distribution, using a stress decomposition technique.
- Determination of the distance away from the weld center at which residual stress vanishes completely, based on component geometry by comparison of data from available literature.
- Comparison of several finite element analyses results from the open literature, covering a broad range of component geometries (r/t ratio), joint preparations (Single V, Double V), materials, and heat input.

2. Guidance on residual stress profiles for assessing flaws in FFS codes

2.1. Residual stress profiles in BS 7910:2019 & R6

BS 7910:2019 [35] is an FFS service code, serving as a "guide to methods for assessing the acceptability of flaws in metallic structures". In 2013, BS 7910 included substantial methods for incorporating welding residual stress into fracture assessment, originating mainly from BS 7910:2005 [18], R6 Revision 4 [16] and the European SINTAP/ FITNET procedures [14,17]. In the 2019 version of BS 7910 [35], no major changes took place in residual stress information, with the exception of the addition of a new Annex, V, on strain-based assessment and design [35]. BS 7910 Clause 7.1 8 states that residual stresses may be assumed to be uniform or non-uniform. Uniform (membrane) stress distributions are considered in this clause, which is more conservative, while non-uniform distributions are described in Annex Q. Annex Q provides guidance on residual stress profiles for assessing flaws in as-welded joints, i.e. joints which are not subjected to post weld heat treatment (PWHT), as shown in Fig. 3.

2.1.1. Transverse residual stress

In BS 7910 Annex Q [35], the transverse residual stress σ_t^r (perpendicular to the weld) has three types of through-thickness distributions, depending on the materials (ferritic versus austenitic) and welding heat input levels, as explained in the equations below.

$$\sigma_t^r(x) = \sigma_Y\left[1 - 6.80\left(\frac{x}{t}\right) + 24.30\left(\frac{x}{t}\right)^2 - 28.68\left(\frac{x}{t}\right)^3 + 11.18\left(\frac{x}{t}\right)^4\right] \quad \text{for } Q'/t \le 50 \text{ J/mm}^2 \tag{4}$$

$$\sigma_t^r(x) = \sigma_Y\left[1 - 4.43\left(\frac{x}{t}\right) + 13.53\left(\frac{x}{t}\right)^2 - 16.93\left(\frac{x}{t}\right)^3 + 7.03\left(\frac{x}{t}\right)^4\right] \quad \text{for } 50 < Q'/t \le 120 \text{ J/mm}^2 \tag{5}$$

$$\sigma_t^r(x) = \sigma_Y\left[1 - 0.22\left(\frac{x}{t}\right) + 3.06\left(\frac{x}{t}\right)^2 + 1.88\left(\frac{x}{t}\right)^3\right] \quad \text{for } Q'/t \ge 120 \text{ J/mm}^2 \tag{6}$$

where Q' represents the linear heat input of the welding electrode for the largest run of the weld. This linear heat input is related to the welding current (I), welding voltage (V) and welding travel speed (u), as per Eq. (7). The through-thickness longitudinal and transverse residual stress profiles given by Eqs. (4)–(6) are plotted in Fig. 4.

$$Q' = \frac{I.V}{u} \tag{7}$$

2.1.2. Residual stress profiles at a distance away from the weld in BS 7910

In the axial direction, BS 7910 specifies that through-thickness residual stress profiles are valid for a region within three times the weld width (3 W) w.r.t the weld centerline, as illustrated in Fig. 5 (a). R6 Sec. IV.4 [16] and FITNET [14] assume a linear distribution of longitudinal

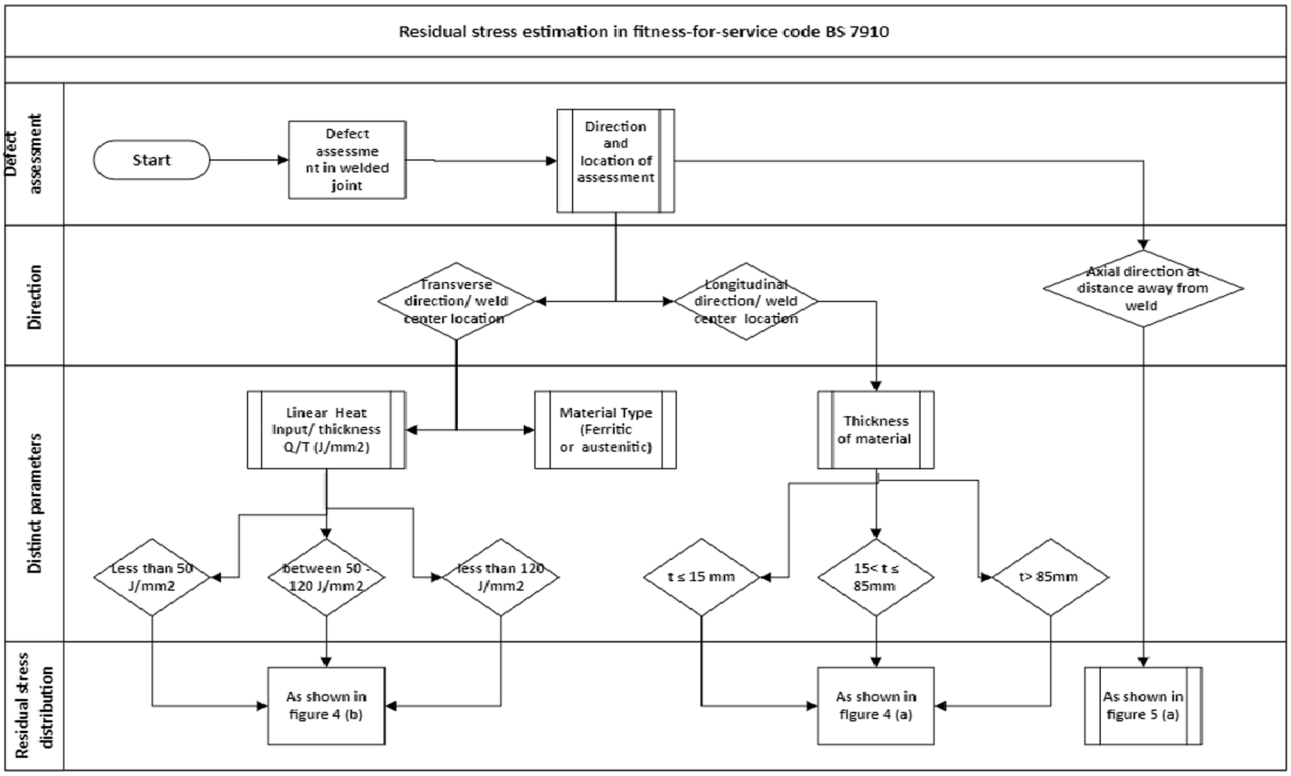

Fig. 3. Residual stress estimation in BS 7910 for welded joints.

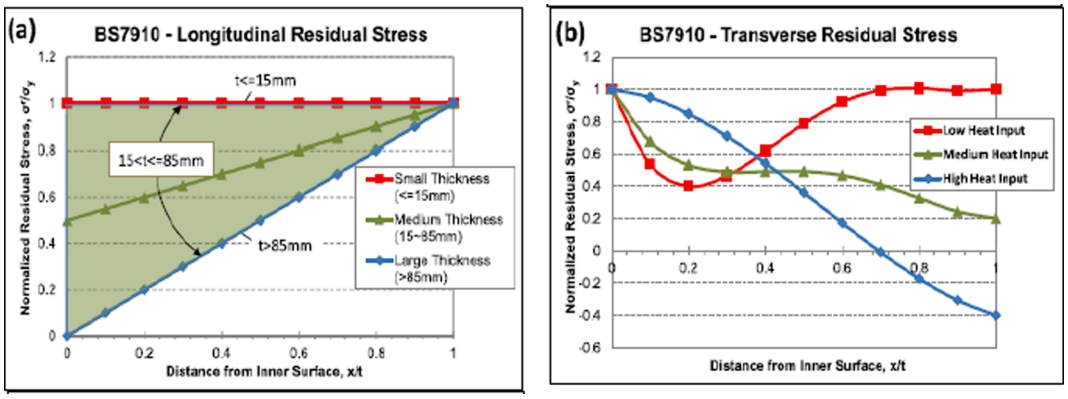

Fig. 4. Residual stress profiles prescribed in BS 7910 Appendix Q [35] and R6 Sec. IV [16]: (a) longitudinal, and (b) transverse directions, adapted from [21] .

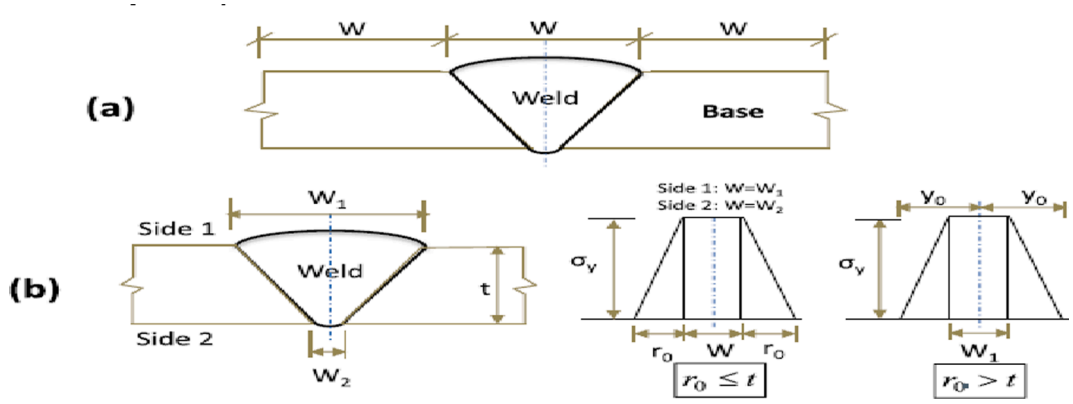

Fig. 5. Illustration of axial residual stress at a distance from weld of surface longitudinal residual stress component: (a) BS 7910 [35], (b) R6 [16], and FITNET [14].

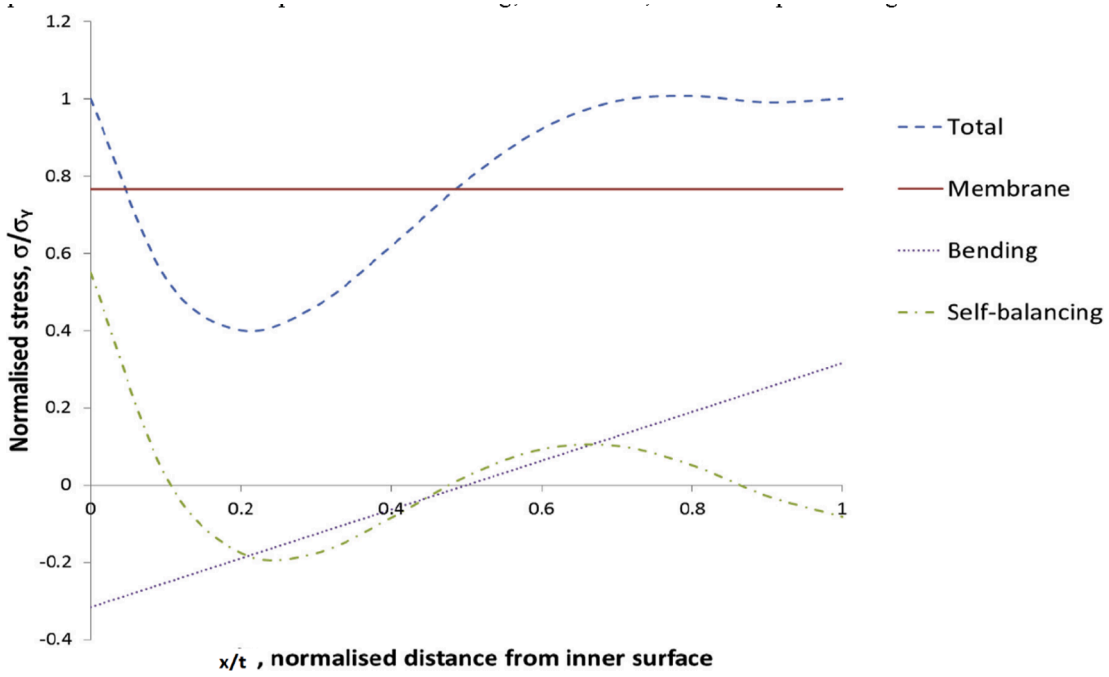

Fig. 6. Decomposed components of transverse stresses in ferritic pipe butt welds (with a low heat input) [31].

residual stress distribution, varying from material yield strength at the weld toe to zero at an estimated yield zone boundary, as illustrated in Fig. 5 (b). All residual stress profiles in BS 7910 are based on upper bound fits to experimental data and FE numerical results. These results are based on different weld geometries measured at weld locations, such as weld centerline and weld toe positions; this does not recognize the role of pipe geometry [36] and is proven to be overly conservative [34]. However, residual stress profiles at a distance away from the weld are not mentioned in FFS structural integrity assessment procedures [19] which can be used in the fracture assessment of proximity welds.

2.1.3. Stress decomposition in BS 7910

As shown in Fig. 6, a stress decomposition technique can be used for depicting a plot of decomposed components of transverse stresses in ferritic pipe butt welds made with a low heat input. The transverse stress $\sigma_t^r(x)$ was calculated from Eq. (4) for low heat input in ferritic pipe butt welds which is normalized to yield strength, σ_Y. This decomposition is shown in Fig. 6, where transverse residual stress normalized by yield strength is plotted against x/t where x is the distance from the inner surface through the wall thickness, t. Eqs. (1)–(3) have been used to calculate and decompose residual stress components into bending, membrane, and self-equilibrating stress.

2.2. API 579-1/ASME FFS-1: Residual stress profile at a distance away from welds

In the case of girth welds, API 2007 579 RP [30] recommends a common curve for axial and hoop residual stress profiles for distances away from the weld toe, based on an upper-bound residual stress profile. The residual stress through-thickness profile at a distance away from the weld is a quadratic variation over a circumferential distance in terms of $\sqrt{rt}$ in API 579 [15], based on a best fit of the upper bound of all finite element results over all r/t ratios and heat inputs. In API 579-1/ASME FFS-1 Annex 9D next update, residual stress profiles for various piping and pressure vessel configurations at distances away from the weld are based on various mechanics-based estimation schemes and the recent research results of Dong and his co-workers [19,34,36,37]. These estimation schemes provide analytically based descriptions of distances at which welding induced residual stress completely vanishes, affected by component geometry (e.g., r/t ratio), shrinkage zone (plastic zone size) controlled by joint preparation and heat input. The key enabler in this process can be attributed to the stress decomposition technique [32] and work done by Dong [19,22,34,38] and Song [21,24,36,37,39,40] in their work to establish a functional dependency of decomposed through-thickness membrane and bending stresses, based on pipe geometry and heat input-related parameters.

3. Review of key contributing parameters governing important residual stress distribution, using stress decomposition technique

To remove the inconsistency in recommended residual stress profiles in various FFS codes, the Pressure Vessel Research Council (PVRC) joint industry project (JIP), Phase 1 [41], was initiated in late 2000, highlighting important parameters affecting upper bound profiles in the 2007 issue of API 579 RP Appendix E [30]. To estimate consistent residual stress profiles, thicknesses of less than 50 mm (2″), mostly for single V joint preparation were used in the phase 1 JIP. Whereas in the phase 2, JIP of PVRC [40] a range of pipe thicknesses between 6.35 mm (1/4″) to 254 mm (10″) with joint preparations of Single V (SV), Double V (DV), and Narrow Groove (NG), were chosen for analysis, as illustrated in Fig. 7.

The outcome of the PVRC JIP, Phase 1 [41], recommended a large number of important governing parameters for estimating residual stress profiles, for example joint geometry, material chemistry, and welding process parameters. However, the role and characteristics of important parameters, such as pipe mean radius to thickness ratio (r/t) and linear heat input (Q), are underestimated in relation to FFS engineering assessment [34]. These distinct parameters affect changes in through-thickness residual stress distributions in the weld center region in the form of a localized distribution (e.g., of the self-equilibrating type). These distributions can be significant at distances away from the weld, which exhibits a “global bending” behavior in the axial residual stress direction [34], i.e. compression of the outer surface and tensile stress on the inside of the pipe geometry. This behavior depicts a decreasing length scale [32], as explained previously in relation to the decomposition technique illustrated in Fig. 2. This technique allows individual identification of residual stress decomposed components which are considered important in defect assessment procedures.

3.1. Component geometry, i.e. radius to thickness (r/t) ratio

Component geometry, such as radius to thickness ratio, serves as a significant distinct parameter having a considerable effect on through-thickness residual stress distribution in weld joints, as demonstrated by researchers like Yaghi [29], Dong [34] and his coworkers [40]. Pipe radial bending stiffness is approximately proportional to $\sqrt{rt}$ [33] , hence r / t ratio serves as an essential measurement criteria for measuring joint restraint conditions.

3.1.1. Demonstrating the effect of component geometry (r/t ratio) at the weld toe location

In this example, the work of Dong [33] and Song [40] sequentially coupled thermo-mechanical analysis based on a conventional heat flow solution for welding are referred [33], where temperature gradients serve as input to nonlinear thermo-mechanical analysis. This example shows the effect of the radius to thickness ratio (r/t) on the through-thickness residual stress profile at the weld center / weld toe region and at a distance away from the weld. The component selected for comparison is the 2.25CrMo-V type [24,29,34], which that is very commonly used in the piping industry. A large number of parametric analyses were performed by Dong [33] and Song [40] for thicknesses > 1″ (25 mm) for pipe to radius ratios (r/t) of 2 to 100; the results demonstrate the effect of the component geometry in estimating

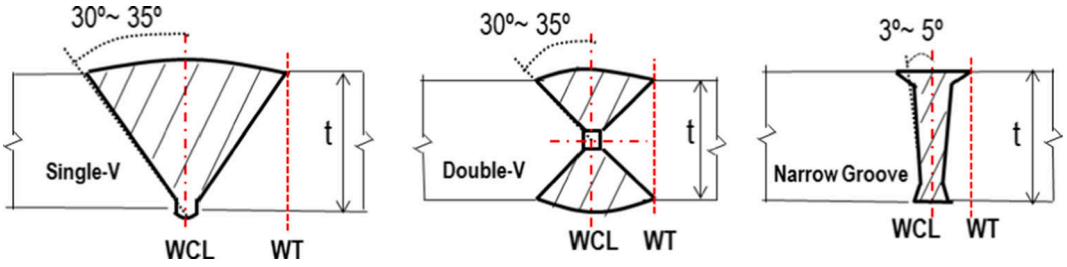

Fig. 7. Illustration of various weld joint configurations investigated in PVRC JIP Phase 2 [40]. Single V (SV), double V (DV), and narrow groove (NG), adapted from [34].

Fig. 8. Residual stress plots (x/t from inner surface) at weld toe locations for Single V & Double V girth welds with t = 1″: r/t ratio effects, adapted from [24].

residual stress profiles. Finite element (FE) results of research work [33] and [40] for single V and double V joint geometry components for thickness of 1″ (25 mm) are illustrated in Fig. 8 for axial and hoop components at the weld toe location. Observations from Fig. 8 are as follows:

- It is evident that axial residual stress for r/t ratio 2 varies from compression at the inner diameter (ID) to tension at the outer diameter (OD), i.e. through-thickness bending mode in the case of a single V joint configuration.
- A shift of compression to tension in the axial direction can be observed at the ID of the pipe, as shown in Fig. 8, as the r/t ratio increases from 2 to 100, starting from r/t = 20, i.e. settling to a self-equilibrating state at r/t = 100 [40]. These bending modes change for a small r/t ratio because the pipe is very stiff at these ratios, while, for a large r/t ratio (e.g. 100), they have increased pipe wall flexibility, i.e. attaining a self-equilibrating component [24].
- As the r/t ratio increases, the lines become flatter at the OD, implying a reduced bending component. Whereas at r/t ratio = 100, residual stress is tensile at ID and OD and a corresponding increased membrane component i.e. tensile at OD. A joint configuration change from single V to double V with an increasing r/t ratio also affects changes in the residual stress profiles, as shown in Fig. 8.

3.1.2. Demonstrating the effect of r/t ratio on residual stress profile at a distance away from weld at outer diameter (OD) and inner diameter (ID)

In Fig. 9, showing residual stress curves on the surface of a pipe along the (ID and OD) for single V girth welds with t = 1 in., reference is made

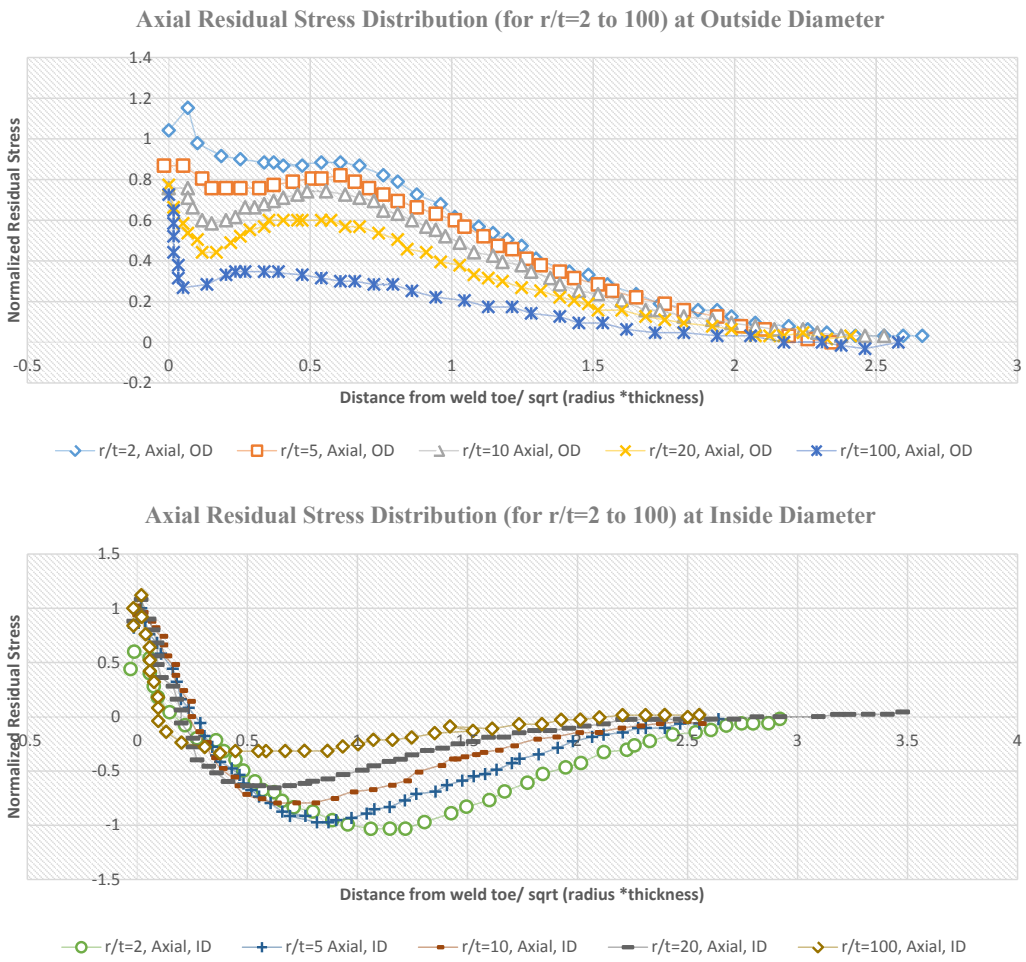

Fig. 9. Surface residual stress line plots along ID and OD for Single V girth welds with t = 1″: r/t ratio effects, adapted from [24].

to r/t ratio effects from the work of Dong[19] and Song [21]. In this comparison, the horizontal axis is a measure from the weld toe and is normalized by $\sqrt{rt}$, which is considered a characteristic parameter in residual stress distribution in the axial direction by PVRC JIP Phase 1 [41] and used in API 579–1/ASME FFS-1 [15]. It can be observed from Fig. 9 that axial residual stress at the OD decreases with increasing r/t ratio and eventually dies to zero at 2.5 times $\sqrt{rt}$. This distance can be considered an important parameter in fracture assessment for flaws away from weld and in proximity to exisitng welds.

3.1.3. Demonstrating the effect of r/t ratio on residual stress profile at a distance from weld in FFS codes

As previously explained, FFS codes [14–16,35] carry practically no recommendations for locations far from the weld center. BS 7910 does not provide any information on through-thickness residual stress profiles in transverse and longitudinal directions, except for the fact that, within the 3 W region, they remain constant (W being the width of the weld seam), as shown in Fig. 5. R6 [16] and FITNET [14], however, recommend a straight line of yield strength in the 0.5 W region (half width of the weld) with a constant residual stress profile, then decreasing it to zero in the longitudinal direction from the weld toe to a distance of r_0, as shown in Fig. 10 (b). In Fig. 10 (a), a comparison of transverse residual stress distributions and (b) longitudinal residual stress distributions along the outer surface (t = 4″, 101.6 mm) is depicted, to showcase the conservativeness associated with FFS codes from the work of Dong [19] and Song [21]. Some observations from Fig. 10 follow.

- It is evident from the results that both BS 7910 [35] and R6/FITNET [14,16] provide less conservative residual stress values within a region of 0.5 W from the weld centerline.
- As shown in Fig. 10, there is an overestimation of longitudinal residual stress at distances beyond 0.5 times the width of weld with prevalent residual stresses for different component geometries [33].
- Beyond the 0.5 W region in the longitudinal direction (Fig. 10 b) residual stress reverses its sign from compression to tension with r/t ratios greater than 2.
- Slope of RG/FITNET curve [14,16] is somewhat large when compared with FE results attained from work of Dong [19] and Song [21] for calculated distance r_o, in longitudinal direction as shown in Fig. 10 b.
- Similarly, for inner surface transverse (not illustrated) the residual stress is overestimated by BS 7910 profile. Longitudinal residual stress estimated by R6/FITNET, the slope is relatively large compared with the FE results.

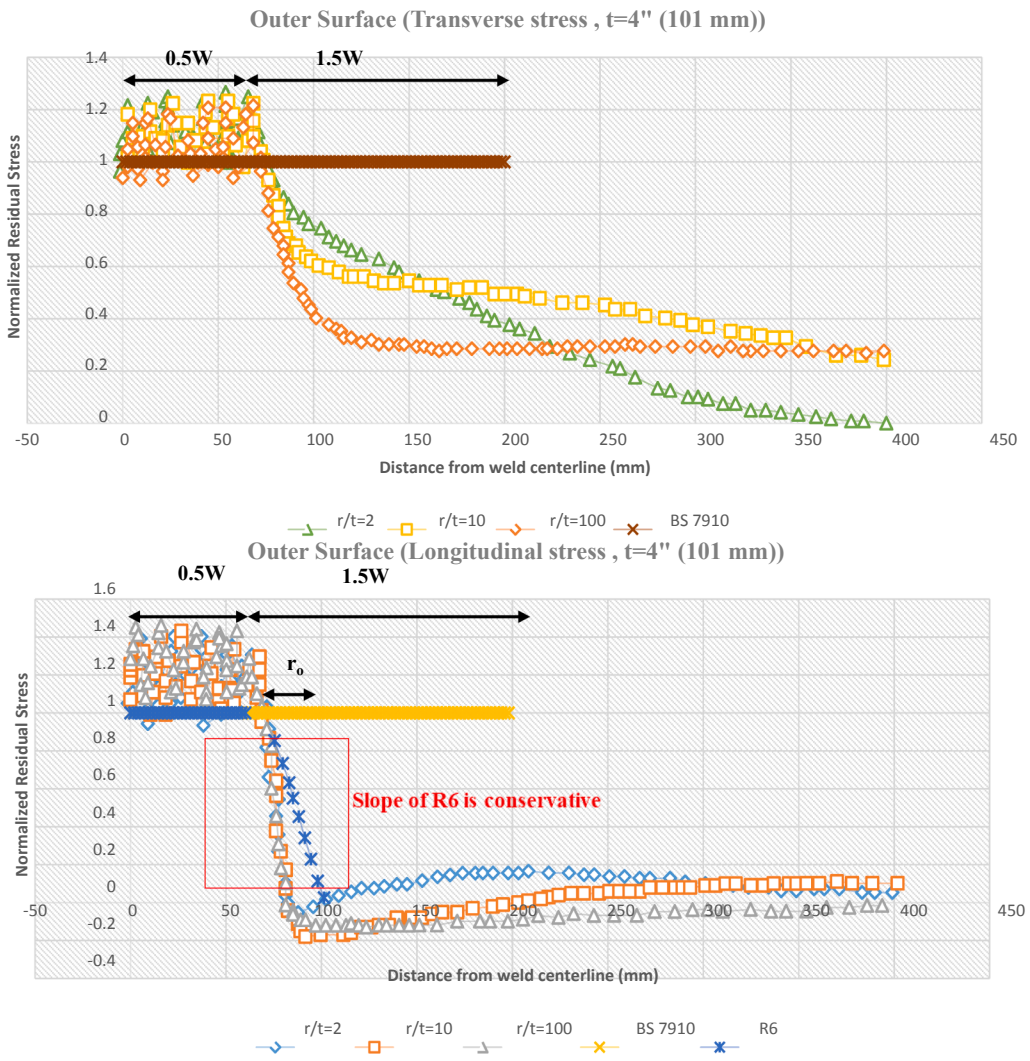

Fig. 10. Comparison of residual stress distributions along outer surface (a) transverse, and (b) longitudinal direction, adapted from [21].

3.1.4. Demonstrating the effect of r/t ratio on residual stress profile using stress decomposition technique

As previously explained, the stress decomposition technique [32] was used by Dong [19] and Song [21] in their work to quantitatively highlight the effect of decomposed components of stress for residual stress distributions. In Fig. 11, decomposed residual stress components at weld toe locations, as a function of r/t ratio for single vee (SV) and double vee (DV) girth welds, are shown, calculated from Eqs. (1)–(3). Observations from Fig. 11 follow.

- In Fig. 11, it can be observed that the decomposed bending component decreases linearly with increasing r/t ratio in the case of axial and hoop residual stresses. This implies a reduced radial restraint as r/t ratio increases, as it measures radial bending stiffness.
- The membrane component is usually negligible in the axial direction (not shown in Fig. 11), unless final assembly welds or severe restraints are present.
- The membrane component of hoop residual stresses increases linearly with increasing r/t ratio.
- This technique recognizes patterns of residual stress distributions at interesting locations (weld toe, weld center, etc.) for all thicknesses, joint configurations (SV, DV) regarding r/t ratio effects.
- The component geometry feature radius to thickness ratio (r/t) clearly highlights membrane and bending components of through-thickness residual stress distributions in the axial and hoop directions.

3.1.5. Demonstrating the effect of thickness on residual stress profile with increasing r/t ratio

In the Phase 1 report of PVRC JIP [41], thickness effect was characterized as an important criterion for residual stress distribution in different weld geometries, as mentioned in Fig. 7, for thicknesses up to 50 mm (2 in.). Phase 2 [40] of PVRC JIP focused on thicknesses from above 50 mm (2 in.) to 250 mm (10 in.) for different weld geometries. As illustrated in Table 1, the effect of thickness on axial residual stress distribution with increasing r/t ratio as mentioned in PVRC JIP Phase1 [41]. It shows that keeping the r/t ratio constant with increasing thickness leads to a global bending type behavior (i.e. compression on the outside and tension on the inner diameter), which changes to local

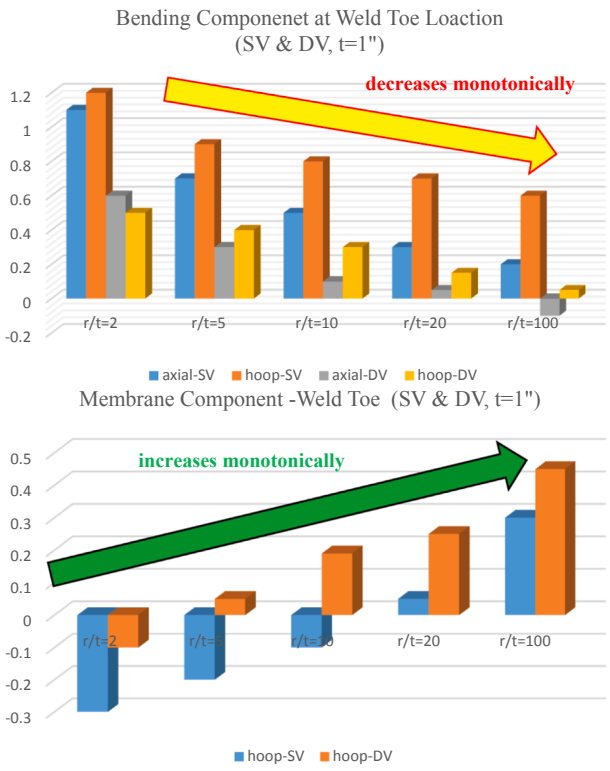

Fig. 11. Residual stress decomposed components at weld toe locations as a function of r/t ratio for Single V (SV) and Double V (DV) girth welds, adapted from [40].

bending (i.e. tension on the outside and compression on the inner diameter). As thickness increases or r/t increases, the bending component changes to a self-equilibrating type [24].

Thickness effects are better characterized in terms of decomposed stress components, as shown in Table 2. The effect of thickness on decomposed stress components with increasing thickness are shown for axial bending, hoop bending and hoop membrane at the weld toe location. The axial and bending hoop components increases between thickness 6.25–25.4 mm (1/4″-1″) and becomes constant for thickness 25.4–250.4 mm (1″–10″) for single and double V weld geometries, whereas, on the other hand, the hoop membrane component decreases with increasing thickness.

3.2. Heat input

As explained previously in Section 2.1.1 (Eq. (7)) and recommended by Phase 1 of the PVRC JIP [41], linear heat input is defined as a product of current, voltage and welding efficiency, divided by travelling speed, with units of J/mm. However, characteristic heat input per unit area (e.g., J/mm^2) or per unit volume (J/mm^3) has demonstrated better ability to highlight residual stress distribution patterns as defined in the PVRC JIP Phase 2 report [40]. Parameter $\dot{Q}$ referred to as characteristic heat input, is defined as follows in Eq. (8).

$$\dot{Q} = \frac{Q'}{A_{pass}} \cdot t_n \tag{8}$$

where A_{pass} is the average pass area and t_n represents weld pass layer thickness. Q' (linear heat input) is further defined in Eq. (9) as the sum of Q'_1 and Q'_2, taking account of additional 3D heat loss ($\eta' = 1.35$). In a 2D heat transfer model for welding [42], a less complicated approach is widely accepted among researchers [29 42], separating heat input into two parts, Q'_1 and Q'_2. Q'_1 represents heat content involved to deposit a molten weld pass at a specified melting temperature and Q'_2 is heat that is required to hold (t_{hold}) the melting temperature shown in Eq. (10) and Eq. (11).

$$Q' = (Q'_1 + Q'_2) \cdot \eta' \tag{9}$$

$$Q'_1 = \rho \cdot C_P \cdot \Delta T \cdot A_{pass} \tag{10}$$

Table 2
Thickness effect on decomposed stress components with increasing thickness [24].

Thickness effect on decomposed stress components with increasing thickness				
At weld toe	Weld Geometry	thickness		
		6.25 mm (1/4″)	25.4 mm (1″)	254 mm (10″)
Axial bending	Single V & Double V	Increases (1/4″-1″)		Constant (1-″10″)
Hoop bending		Increases (1/4″-1″)		Constant (1-″10″)
Hoop membrane		decreases		

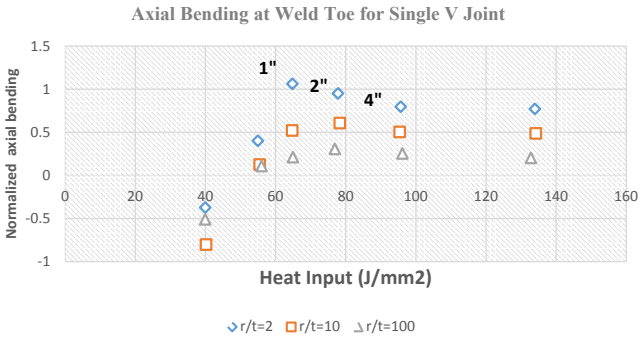

Fig. 12. Decomposed axial bending residual stress components at weld toe as a function of characteristic heat input for SV girth welds, adapted from [24].

Table 1
Thickness effect on axial residual stress distribution, adapted from [24].

Thickness effect on axial residual stress distribution with increasing r/t ratio							
r/t ratio		Thickness (mm)				Axial residual stress	Weld geometry
2		25	50	100	250	Changes global to local bending	Single Vee
10		Thickness increase while r/t constant				Local bending is gradually transitioned to self-equilibrating type	Single Vee
20							Single Vee
100		Thickness and r/t increases					Single Vee

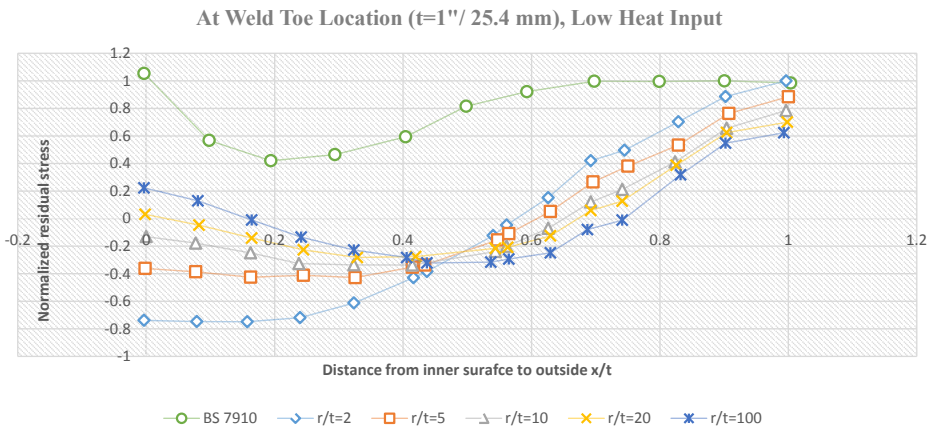

Fig. 13. Transverse residual stresses for low heat input cases t = 1″ (25.4 mm) at weld toe for different r/t ratios, adapted from [19].

$$Q_2^{\cdot} = 2k \cdot \Delta T \cdot \sqrt{\frac{t_{hold}}{\pi\alpha}} \cdot L_S \tag{11}$$

2D heat transfer models have a limitation of leaving heat loss in the third direction; hence, careful establishment must be applied between the heat input implied in the 2D cross-section models (e.g., axisymmetric or generalized plane strain models) and the linear heat input (Eq. (7)) used in practice [34]. The linear heat input parameter defined in Eq. (7), with units of J/mm, badly underestimates residual stress distributions in correlating different heat input conditions, as proven in investigations by Bouchard [23] and Dong [22]. In Phase 2 of the PVRC JIP, where a wide range of geometries and welding processes were investigated by Dong [22] and his co-workers [40], heat input $\dot{Q}$, mentioned in Eq. (8), was proposed as the characteristic heat input parameter for correlating through-thickness membrane and bending stress components.

3.2.1. *Decomposed residual stress components in heat input*

Characteristic heat input $\dot{Q}$, as defined in Eq. (8), is effective in correlating a large number of residual stress distributions related to r/t ratio and thickness effects, as proposed by Dong and his co-workers [39]. Decomposed residual stress components at the weld toe location are shown in Fig. 12, as a function of characteristic heat input$\dot{Q}$ for single V girth welds, as mentioned in the PVRC JIP Phase 2 report [40] for axial bending, hoop membrane and hoop bending components. In this example, $\dot{Q}$ (J/mm2), the heat input per unit of the weld layer cross-section area, was calculated from Eq. (8), in which Q' stands for linear heat input which can be calculated by using Eq. (10) and Eq. (11). Fig. 12 depicts decomposed normalized axial bending residual stress at the weld toe location for single-V girth welds as a function of characteristic heat input $\dot{Q}$ (J/mm^2). This demonstrates the ability to distinguish the effects of r/t ratio and thickness for the residual stress distribution of pipe girth welds. Similar results were also demonstrated for hoop membrane and bending components in the PVRC JIP Phase 2 report [40]. Characteristic heat input parameter$\dot{Q}$ (J/mm^2) can be directly related to weld shrinkage force in the hoop direction, as the maximum membrane hoop stress of yield magnitude exerts the maximum circumferential shrinkage force, causing the strongest axial bending stress, as demonstrated in the work of Song [39]. Thus, characteristic heat input parameter$\dot{Q}$ serves as an important driving force for highlighting the bending component of the axial residual stress.

3.2.2. *Role of heat input in FFS codes (BS 7910) at weld toe location*

As defined in Eqs. (4)–(6) and illustrated in Fig. 4, transverse residual stress in BS 7910 is divided into 'high' (heat input > 120 J/mm^2), 'low' (heat input ≤ 50 J/mm^2) and 'medium' (heat inputs between 50 and 120 J/mm^2). From the work of Dong [19], the results of parametric analysis are illustrated in Fig. 13 on 2¼ Cr-Mo-V steel for wall thickness 25.4 mm (1 in.) in low heat input at the weld toe location. BS 7910 provides an upper bound estimate of residual stress distributions as per Eq. (4). It can be clearly observed that, from Fig. 13, the BS 7910 profiles for low heat input become more conservative as the r/t ratio becomes smaller (r/t = 2) at the weld toe location. A noticeable effect is observed on the inside surface compared to the outer surface of the pipe.

In Figs. 14 and 15, transverse residual stress distributions for medium and high heat input for wall thicknesses of ¼ inches (6.35 mm) and 1 in. (25.4 mm), respectively, at the weld toe location are depicted from the work of Dong [19], to illustrate the conservatism associated with BS 7910. At the outer surfaces, with increasing r/t ratio, residual stresses are significantly lower. Transverse residual stress at the inside diameter of the pipe is close to yield strength, whereas the stress at the outer diameter is reduced to approximately 25% of yield strength for the case of medium heat input.

4. Complete residual stress profile estimation scheme at a distance away from weld

As reviewed and explained in earlier sections, pipe (r/t) ratio and characteristic heat input parameter$\dot{Q}$ serve as key parameters in estimating residual stress profiles applicable for wide weld geometries and welding conditions. In Eqs. (1)–(3), using stress decomposition technique clearly defines decomposed components of residual stress at girth weld locations in terms of bending, membrane and self-equilibrating, which can be further expressed as Eq. (12) and illustrated in Fig. 16.

$$\frac{\sigma_r(\varepsilon)}{\sigma_y} = \bar{\sigma_m} + \bar{\sigma_b}\varepsilon + \bar{\sigma_{se}}(\varepsilon) \tag{12}$$

where ε is a dimensionless factor, expressed as$\varepsilon = 2\left(\frac{x}{t}\right) - 1$, x measured

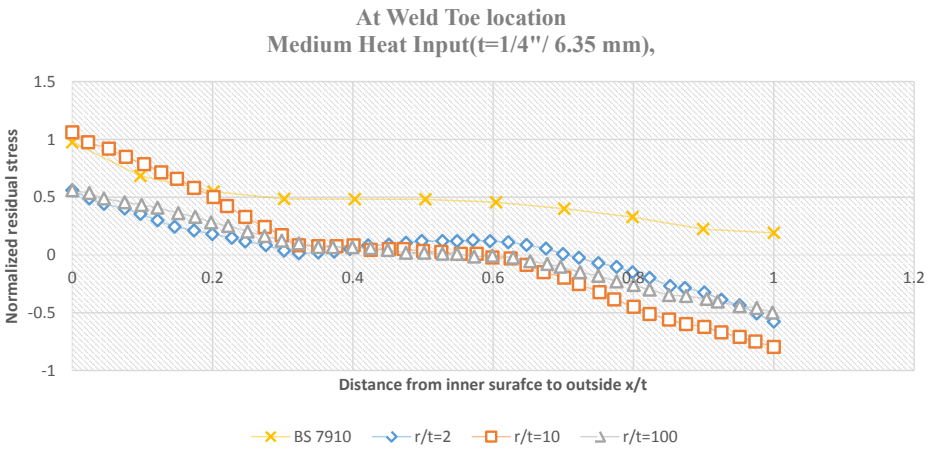

Fig. 14. Transverse residual stresses for medium heat input cases (t = 1/4″ (6.35 mm)) at weld toe for different r/t ratios, adapted from [19].

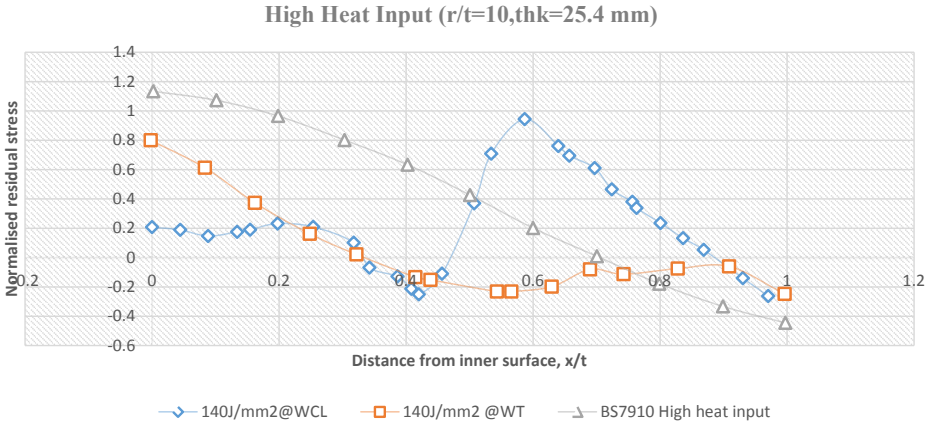

Fig. 15. Comparison of transverse residual stresses for high heat input cases (t = 1″, 25.4 mm), adapted from [19].

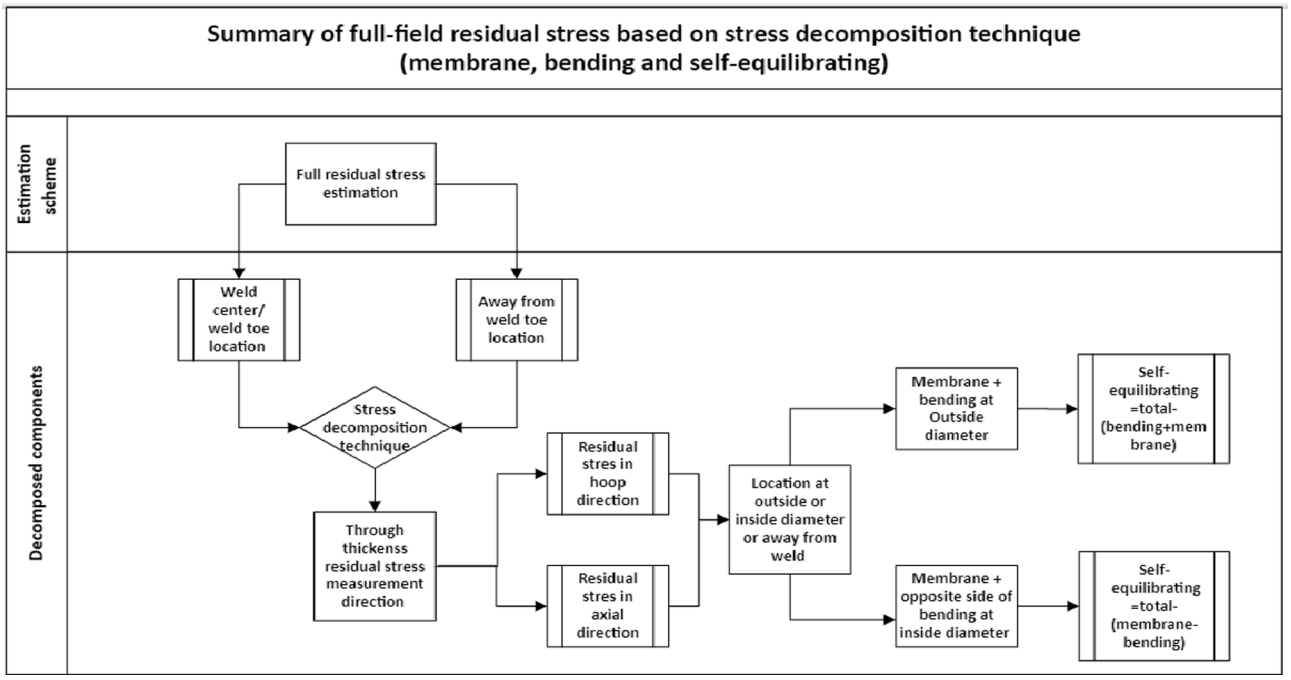

Fig. 16. Full residual stress estimation scheme, adapted from [24].

from the inside of the pipe to the outside, and $\sigma_y$is the yield strength of the material.

At a distance away from the weld, the residual stress estimation shell theory-based estimation scheme [43] proposed by Song and Dong [19,37] is referred. This theory was introduced by Song and Dong [19,37] to quantify the effect of restraint on residual stress estimation through thickness profiles for distances or positions along the axial direction of the pipe. Bending and membrane components of through-thickness residual stress profiles are known to contribute equally towards the crack driving force at distances away from the weld [19,32,38], in contrast to the self-equilibrating component. The role of component geometry like radius to thickness ratio, weld geometry configurations such as single or double Vee joints, heat input and material effects are well established in this scheme for estimating accurate residual stress distribution at distances away from the weld.

The use of the shell theory-based estimation scheme [43] has been found to produce conservative results [37] for thicknesses ranging from 6.25 to 100 mm and different weld joint configurations having varying r/t ratios between 10 and 100. This scheme has the advantage of estimating less conservative residual stress components at distances away from the weld, in terms of stress decomposition components, and highlighting the role of crack driving components, i.e. membrane and bending. Another advantage of using this scheme is the estimation of radial distortion in welded thick sections. This scheme can be used efficiently in the defect assessment of proximity girth welds.

5. Conclusion

In this manuscript, a detailed review is presented of residual stress estimation in fitness-for-service codes (FFS) like BS 7910, R6 & API 579 used in the defect assessment of welded components. Available profiles in these FFS codes are based on the results of the residual stress measurement technique coupled with finite element analysis results. Due to large variations in measurement techniques, modeling methods and the complex nature of welding, the residual stress profiles recommended in these FFS codes at the weld center or weld toe region are found to be overly conservative. Residual stress estimation schemes at a distance away from the weld recommended in these codes have been found to be practically nonexistent or overly conservative. BS 7910 has a constant transverse residual stress profile in 1.5 W region from the weld centerline, where W is weld width. Beyond this region, there are no prevalent recommendations in the BS 7910 code. R6 and FITNET assume a linear distribution of longitudinal residual stress distribution varying from material yield strength at the weld toe to zero at an estimated yield zone boundary. API 579, however, provides a single curve-based upper-bound estimate of axial and hoop residual stress profiles for locations away from the weld toe. This clearly highlights the overconservativeness brought by these codes while assessing residual stress at a distance away from the weld for application scenarios like proximity welds for the defect assessment of welded structural joints and piping joints, where the superposition of residual stresses can take place.

The stress decomposition technique, a length scale-based characterization, was introduced by Dong and his co-workers, decomposing residual stress components into membrane, bending and self-equilibrating stresses, corresponding to decreasing length scale. The introduction of this technique in the BS 7910 FFS code has been found useful in separating the contribution of global and local residual stress and visualizing better patterns of residual stress distribution and analyzing many residual stress cases to identify the controlling parameters. However, residual stress distribution at a distance away from welds exhibits a “global bending” behavior in the axial residual stress direction, i.e. compression of the outer surface and tensile stress on the inside of the pipe geometry, which provides valuable analysis in defect assessment procedures. For the development of consistent residual stress profiles prescribed in the FFS codes, the Phase 1 & 2 reports of the Pressure Vessel Research Council’s (PVRC) joint industry project (JIP) analyzed key contributing factors like material effects, thickness (t), weld pass, etc., of which the component geometry feature, pipe mean radius to thickness ratio (r/t), and the characteristic heat input, (per unit volume) ($\dot{Q}$), has shown a functional dependency of decomposed through-thickness membrane and bending stresses. Key important features like component geometry (e.g., r/t ratio), shrinkage zone (plastic zone size), controlled by joint preparation and heat input, highlight the important residual stress profiles for various piping and pressure vessel configurations. The research findings of Dong and his co-workers are under consideration to be adopted as part of the API 579 FFS codes’ revisions for residual stresses, comprising various mechanics-based estimation schemes for distances away from the weld.

While determining full residual stress profiles at the weld center and toe regions by use of the stress decomposition technique, membrane and bending components have been shown to contribute significantly towards the determination of the crack driving force, in contrast to the low contribution of the self-equilibrating component. However, at a distance away from the weld, shell theory recommended from the research results of Song and Dong provides consistent through-wall residual stress distributions in terms of bending and membrane components. The role of component geometry, such as radius to thickness ratio and heat input, is well established in this scheme for estimating accurate residual stress distribution at distances away from the weld. The use of machine learning algorithms based on input data from the results of FE analysis, coupled with experiments on selected components with varying geometries and welding processes, can help in developing application guidance tools for predicting accurate residual stress profiles on welded joints at distances away from the weld.

CRediT authorship contribution statement

Sachin Bhardwaj: Conceptualization, Investigation, Methodology, Visualization, Writing - original draft, Writing - review & editing. **R.M. Chandima Ratnayake: . :** Conceptualization, Formal analysis, Funding acquisition, Project administration, Supervision.

Declaration of Competing Interest

The authors declare that they have no known competing financial interests or personal relationships that could have appeared to influence the work reported in this paper.

Acknowledgment

This work has been carried out as part of a PhD research project, performed at the University of Stavanger, Norway. The research is fully funded by the Norwegian Ministry of Education.

Appendix A. Proposal for estimating residual stress profile at weld toe and away locations on girth welds

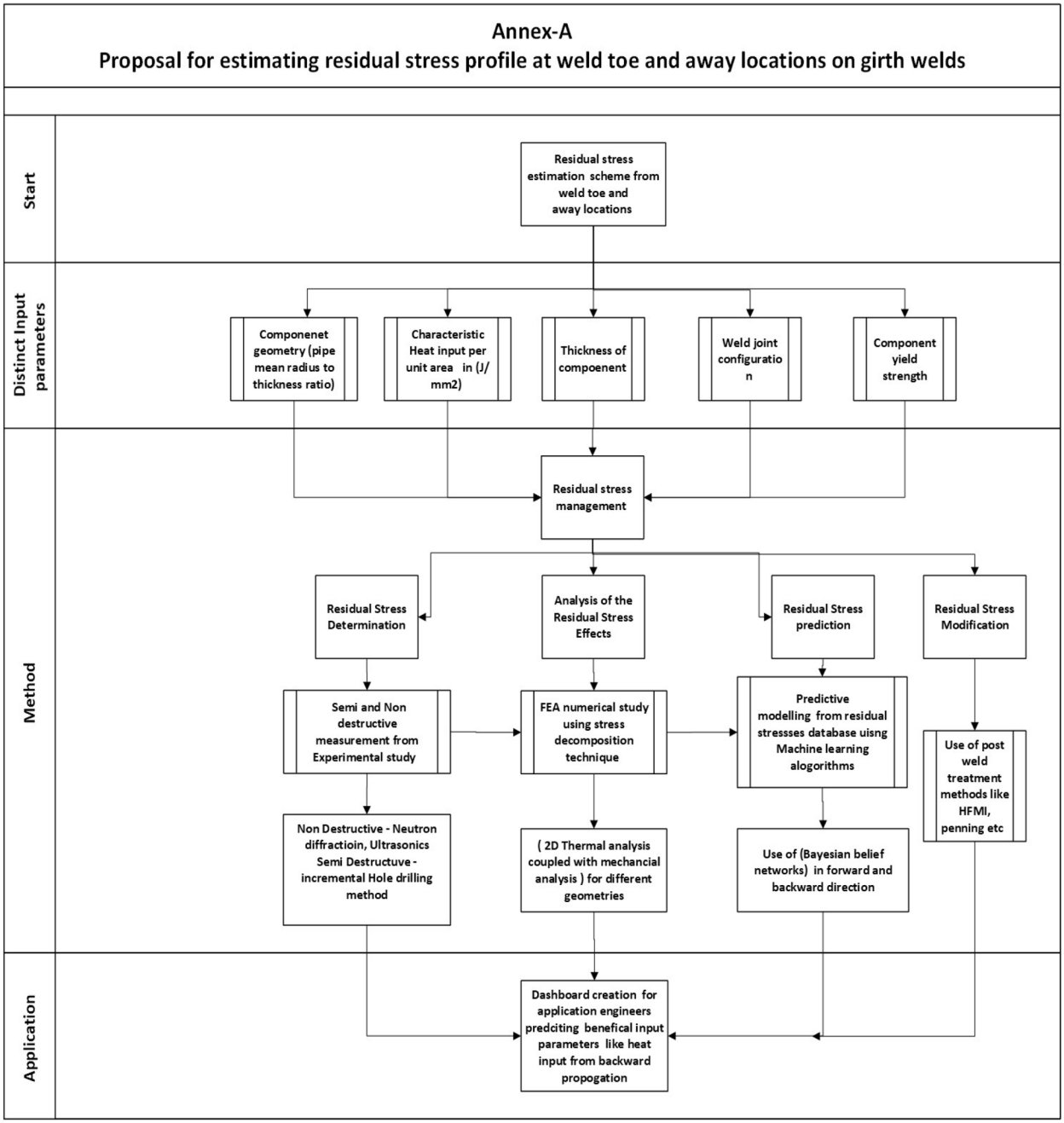

References

[1] R.M.C. Ratnayake, V.A. Brevik, Experimental investigation of underwater stud friction stir welding parameters, Mater. Manuf. Processes 29 (10) (2014) 1219–1225.

[2] R.M. Ratnayake, et al., Underwater friction stud welding optimal parameter estimation: engineering robust design based approach, J. Offshore Mech. Arct. Eng. 137 (2015).

[3] R.M. Ratnayake, D. Dyakov, Optimal arc welding process parameter combination design and metallographic examination for SDSS Butt Welds, J. Offshore Mech. Arct. Eng. 139 (2017).

[4] R.M. Ratnayake, An algorithm to prioritize welding quality deterioration factors: A case study from a piping component fabrication process, Int. J. Qual. Reliab. Manage. 30 (2013).

[5] R.M. Ratnayake, A methodology for assessing most vulnerable welding procedure specifications and imperfection factors, Int. J. Data Anal. Tech. Strategies 6 (2014) 362–383.

[6] S. Bhardwaj, R.M.C. Ratnayake, Challenges due to welds fabricated at a close proximity on offshore structures, Pipelines, And Piping: State Of The Art, in: OMAE2020, ASME, Editor, 2020, ASME: OMAE2019-18586.

[7] Larsson Magnus, L. Mattias, R.M.C. Ratnayake. Investigation of fatigue strength behaviour in dual weld S420 steel joints fabricated at a close proximity, in: Proceedings of 1st International Conference on Structural Damage Modelling and Assessment. Lecture Notes in Civil Engineering, vol. 110, 2020.

[8] Larsson Magnus, L. Mattias, R.M.C. Ratnayake, Experimental investigation of weld joints manufactured at close proximity in S420 structural steel, in: Proceedings of 1st International Conference on Structural Damage Modelling and Assessment. Lecture Notes in Civil Engineering. Vol 110, 2020.

[9] Larsson Magnus, L. Mattias, X. Ficquet, R.M.C. Ratnayake, Experimental Residual Stress Investigation of Weld Joints Fabricated at a Close proximity in S420 Structural Steel. Proceedings of 1st International Conference on Structural Damage Modelling and Assessment. Lecture Notes in Civil Engineering. Vol 110, 2020.

[10] S.K. Bate, et al., A review of residual stress distributions in welded joints for the defect assessment of offshore structures. Offshore technology report. Vol. OTH 482, 1998, Sudbury: HSE Books.
[11] B. Brickstad, B.L. Josefson, A parametric study of residual stresses in multi-pass butt-welded stainless steel pipes, Int. J. Press. Vessels Pip. 75 (1) (1998) 11–25.
[12] M. Law, et al., Residual stress measurements in coil, linepipe and girth welded pipe, Mater. Sci. Eng., A 437 (1) (2006) 60–63.
[13] M.N. James, et al., 10 - Assessing residual stresses in predicting the service life of welded structures, in: K.A. Macdonald (Ed.), Fracture and Fatigue of Welded Joints and Structures, Woodhead Publishing, 2011, pp. 276–296.
[14] FITNET, European Fitness-for-service Network, 2006.
[15] American Petroleum Institute, API 579-1/ASME FFS-1.Appendix E, Houston, TX: American Petroleum Institute: USA, 2016.
[16] British Energy Generation Ltd, Procedure R6 revision 4, assessment of the integrity of structures containing defects, UK, 2013.
[17] SINTAP, Structural Integrity Assessment Procedures for European Industry, BriteEuRam Project Final Report, 1999.
[18] British Standard, BS 7910:2005: Guide to methods for assessing the acceptability of flaws in metallic structures, 2005,: UK. p. 535.
[19] P. Dong, et al., On residual stress prescriptions for fitness for service assessment of pipe girth welds, Int. J. Press. Vessels Pip. 123–124 (2014) 19–29.
[20] A. Mirzaee-Sisan, G. Wu, Residual stress in pipeline girth welds- A review of recent data and modelling, Int. J. Press. Vessels Pip. 169 (2019) 142–152.
[21] S. Song, P. Dong, J. Zhang, A full-field residual stress profile estimation scheme for pipe girth welds, vol. 9, 2012.
[22] P. Dong, J.K. Hong, On the residual stress profiles in new API 579/ASME FFS-1 Appendix E, Welding in the World 51 (5) (2007) 119–127.
[23] P.J. Bouchard, Validated residual stress profiles for fracture assessments of stainless steel pipe girth welds, Int. J. Press. Vessels Pip. 84 (4) (2007) 195–222.
[24] S. Song, Analysis and characterization of residual stresses in pipe and vessel welds, in: Naval Architecture and Marine Engineering, University of New Orleans New Orleans, USA, 2012.
[25] Ali Mirzaee-Sisan, P.J.B., Foroogh Hosseinzadeh, Standardisation on Measurement and Interpretation of Residual Stress Data, in OMAE2019, ASME, Editor, ASME: OMAE2019-96615, 2019.
[26] P.J. Bouchard, Code characterisation of weld residual stress levels and the problem of innate scatter, Int. J. Press. Vessels Pip. 85 (3) (2008) 152–165.
[27] A. Yaghi, et al., A comparison between measured and modeled residual stresses in a circumferentially butt-welded P91 steel pipe, J. Pressure Vessel Technol. 132 (2010).
[28] A. Yaghi, et al., Residual stress simulation in thin and thick-walled stainless steel pipe welds including pipe diameter effects, Int. J. Press. Vessels Pip. 83 (11) (2006) 864–874.
[29] A.H. Yaghi, et al., Residual stress simulation in welded sections of P91 pipes, J. Mater. Process. Technol. 167 (2) (2005) 480–487.
[30] American Petroleum Institute, API RP 579, Houston, TX: American Petroleum Institute; August 2007, USA, 2007.
[31] J. Sharples, I. Hadley, Treatment of residual stress in fracture assessment: background to the advice given in BS 7910:2013, Int. J. Press. Vessels Pip. 168 (2018).
[32] P. Dong, Length scale of secondary stresses in fracture and fatigue, Int. J. Press. Vessels Pip. 85 (3) (2008) 128–143.
[33] P. Dong, Recommendations for determining residual stresses in fitness-for-service applications, Welding Res. Council Bull. (2002) 1–61.
[34] P. Dong, S. Song, X. Pei, An IIW residual stress profile estimation scheme for girth welds in pressure vessel and piping components, Welding World 60 (2) (2016) 283–298.
[35] British Standard, BS 7910:2019: Guide to methods for assessing the acceptability of flaws in metallic structures, 2019, UK. p. 535.
[36] S. Song, P. Dong, A framework for estimating residual stress profile in seam welded pipe and vessel components Part II: Outside of weld region, Int. J. Press. Vessels Pip. 146 (2016) 65–73.
[37] S. Song, P. Dong, X. Pei, A full-field residual stress estimation scheme for fitness-for-service assessment of pipe girth welds: Part II – A shell theory based implementation, Int. J. Press. Vessels Pip. 128 (2015).
[38] P. Dong, F. Brust, Welding residual stresses and effects on fracture in pressure vessel and piping components: a millennium review and beyond, J. Pressure Vessel Technol.-Trans. ASME – J. Pressure Vessel Technol. 122 (2000).
[39] S. Song, P. Dong, A framework for estimating residual stress profile in seam-welded pipe and vessel components part I: Weld region, Int. J. Press. Vessels Pip. 146 (2016) 74–86.
[40] S. Song, P. Dong, X. Pei, A full-field residual stress estimation scheme for fitness-for-service assessment of pipe girth welds: Part I - Identification of key parameters, Int. J. Press. Vessels Pip. 126–127 (2015) 58–70.
[41] P. Dong, Z. Cao, J.K. Hong, Final PVRC Residual Stress and Local PWHT JIP Report on Investigation of Weld Residual Stresses and Local Post Weld Heat Treatment, Phase I, 2005.
[42] S. Song, X. Pei, P. Dong, An analytical interpretation of welding linear heat input for 2D residual stress models, in: ASME 2015 Pressure Vessels and Piping Conference, 2015.
[43] S. Timoshenko, Theory of Plates and Shells, McGraw-Hill Inc., 1959.